A NOVEL SOLUTION FOR THE SPACECRAFT MIXED ACTUATORS PROBLEM BASED ON A MULTIOBJECTIVE OPTIMIZATION METHOD

Willer Gomes dos Santos[(1)], Evandro Marconi Rocco[(2)], Toralf Boge[(3)], Heike Benninghoff[(4)], and Florian Rems[(5)]

[(1)(2)]*National Institute for Space Research (INPE), Av. dos Astronautas 1758, São José dos Campos, Brazil, willer.gomes@inpe.br*

[(3)(4)(5)]*German Aerospace Center (DLR), Münchner Strasse 20, Wessling, Germany*

Abstract: *In this paper, a novel solution for the mixed actuators problem is proposed. This approach uses a multiobjective optimization technique for commanding a group of actuators (thrusters, reaction wheels and magnetic torqrods) simultaneously optimizing a set of objective functions. The multiobjective problem is formulated using combinatorial combinations of the control signal for composing the decision space. The proposed model, called Actuator Multiobjective Command Method (AMCM), is included in a complete guidance, navigation and control loop applied to the final approach rendezvous scenario. Its performance, compared to different actuators configurations, has been evaluated in numerical simulations. In addition, AMCM has been integrated and tested in the hardware-in-the-loop rendezvous and docking simulator of the German Aerospace Center. Results have indicated effectiveness and robustness in both purely numerical and real-time simulations.*

Keywords: *Mixed Actuators Problem, Multiobjective Optimization, Final Approach Rendezvous.*

1. Introduction

Every rendezvous in space aims at carrying out safe, reliable and efficient maneuvers. To meet these requirements, new sensors, actuators and Guidance, Navigation and Control (GNC) methods have to be developed. The challenge of commanding efficiently and autonomously spacecraft actuators has motivated the investigation of new optimization techniques in order to extend the spacecraft's life and to insure the fulfillment of all mission requirements. Over the past years, the spacecraft control problem by using mixed actuators has been the subject of extensive study in several space missions [1, 2]. A mixed actuators mode is a hybrid approach to control the spacecraft using a combination of actuators. A hybrid attitude control mode might be used, for example, as a contingency means for controlling a spacecraft that has lost one or more of its operating reaction wheels. The first NASA Spacecraft Hybrid Attitude Workshop, held in Maryland in April of 2013, aimed to better understand the technical challenges, risks, and benefits of a potential hybrid attitude control mode operations on their science mission spacecraft [3]. Some examples include Kepler, Dawn, Mars Odyssey and Cassini space missions.

In this sense, the problem of optimally and autonomously commanding a group of actuators with conflicting characteristics is explored in this paper and widely discussed in [4]. Thus a novel actuators command strategy based on a discrete multiobjective optimization method has been proposed herein. Such methodology, called Actuator Multiobjective Command Method (AMCM), is responsible for commanding the necessary torque for the actuators at every control cycle according to the torque level requested by the controller. AMCM generates a set of feasible solutions and selects, based on a decision making method, the best compromise solution optimizing

simultaneously a group of objective functions. The proposed approach has been tested in a final approach rendezvous scenario. Due to the complexity of this phase, all elements of the GNC loop have been accurately implemented in a simulation framework. Furthermore this paper also presents results of hardware-in-the-loop (HIL) tests performed on the robotic rendezvous and docking simulator of the German Aerospace Center (DLR), called European Proximity Operations Simulator (EPOS).

2. The Guidance, Navigation and Control Loop

The motion of the final approach rendezvous of two satellites (chaser and target) has been simulated by numerical models. The spacecraft's position and velocity is calculated in the Clohessy-Wiltshire coordinate frame [5] with the origin located in the center of mass (CoM) of the target vehicle. In this coordinate system, the X axis (V-bar) points along the orbital velocity vector, Z axis (R-bar) is radial from the spacecraft CoM to the center of the Earth, and Y axis (H-bar) points in the opposite direction of the angular momentum vector of the orbit. A closed-loop controlled straight line trajectory strategy (along V-bar) has been used to achieve docking capture conditions. The attitude motion is calculated in the body coordinate frame with the origin in the CoM of the chaser spacecraft and with the X axis pointing in the direction of the docking axis. The complete block diagram of the GNC loop can be seen in Fig. 1.

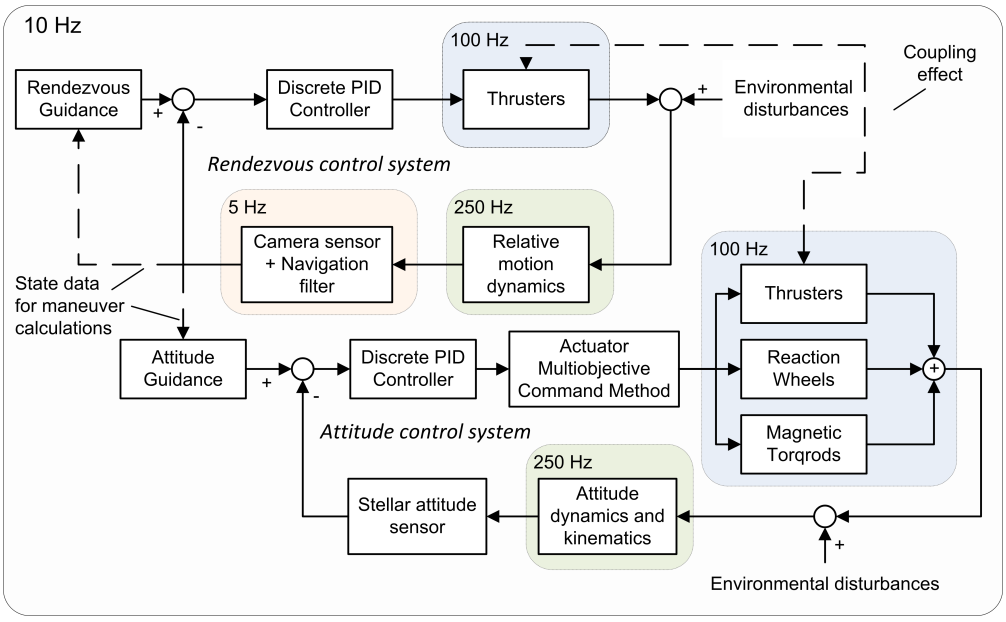

Figure 1. Block diagram of the rendezvous and attitude GNC loop.

The attitude control system is composed of thrusters, reaction wheels and magnetic torqrods whereas the rendezvous control system includes thrusters in a Reaction Control System (RCS) configuration. An usual GNC loop has a operating frequency of 10 Hz [5]; the spacecraft dynamics motions are driven according to the robotic simulator frequency (250 Hz) [6]; the image processing and pose estimation require more computational effort, hence they only provide an update rate of 5 Hz [7]; since actuators have to operate faster than the duty cycle for achieving an accurate attitude control and to allow a pulse width modulated input signal [8, 9], a frequency of 100 Hz has been assumed

for these models. The chaser's relative translational motion is expressed by Hill equations whereas the nonlinear rotational dynamics of the spacecraft is described by Eulers equations [5]. The attitude kinematics is computed using Euler angles (3-2-1 transformation) and quaternions [7]. In addition, two types of external disturbances have been considered in this paper: residual atmospheric drag [10] and gravity gradient moments [8].

Position and attitude profiles are generated, at each sample time, by the guidance subsystems. The attitude guidance subsystem computes over time the necessary rotation to keep the chaser body frame aligned with the target docking axis whereas the rendezvous guidance function calculates the acceleration profile used to achieve the desired approach velocity. This profile comprises a constant acceleration phase, a constant velocity phase, and a constant deceleration phase [5]. The desired values are compared with the estimated values provided by the navigation subsystem which includes a camera sensor, modeled as a pinhole model [6, 11], and an extended Kalman filter [7]. For both attitude and rendezvous sensor models, uniformly distributed random noise and bias have been assumed.

The discrete Proportional-Integral-Derivative (PID) controller [12] has been designed to have a good noise rejection capability, to ensure the stability of the GNC loop, and to keep low steady state errors. The actuator models convert the control signal to forces and torques to be applied in the orbit dynamics and kinematics models. The RCS [5] is used for controlling the translational and rotational motions simultaneously. A pulse width pulse frequency (PWPF) modulation technique [8] has been applied in order to have a varying amplitude thruster control. Minimum Impulse Bit (MIB) is a thruster specification which represents the lower limit of pulse duration. The feasible set of firing duration commands is achieved based on the solution of a linear equation system, such as

$$\mathbf{F} = \mathbf{A}\mathbf{x} \tag{1}$$

where $\mathbf{F} \in \mathbb{R}^6$ is the requested control vector composed of three components of force and torque, respectively; since n is the number of thrusters, then $\mathbf{A} = [A_1, A_2, \cdots, A_n] \in \mathbb{R}^{6\times n}$ is the configuration matrix where its columns $A_i = [f_{ix}, f_{iy}, f_{iz}, t_{ix}, t_{iy}, t_{iz}]^T$ (i = 1, 2, ..., n) define the force and torque components of the thrusters based on their positions and orientations in the body coordinate frame; and $\mathbf{x} = [x_1 \cdots x_n]^T \in \mathbb{R}^n$ is a normalized vector which represents the firing duration commands. In this paper, the RCS setup is composed of 12 thrusters with locations and orientations as shown in Fig. 2.

The reaction wheel is modeled as a flywheel powered by an electromechanical motor. By adjusting the motor input voltage, the flywheel is accelerated or slowed down generating, by reaction, an opposite torque applied to the satellite. Nonlinear friction disturbances inherent to the nonlinear physical characteristics of the electric motor are mainly responsible for causing the error between the commanded and the applied torque. It is assumed three identical reaction wheels with axes of rotation aligned to the body axes frame. Figure 3 presents the electromechanical model of a reaction wheel.

In this model, T_c is the torque command of the controller; K_t is the flywheel torque coefficient; R_w

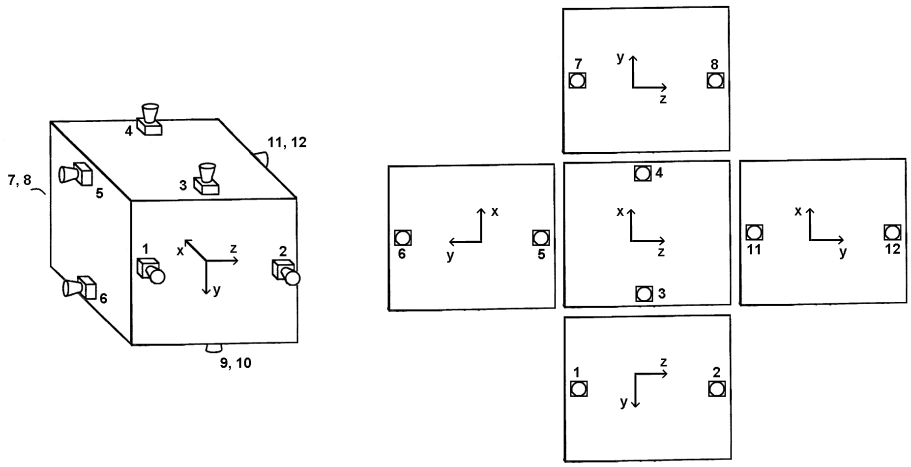

Figure 2. RCS setup for configuration with 12 thrusters.

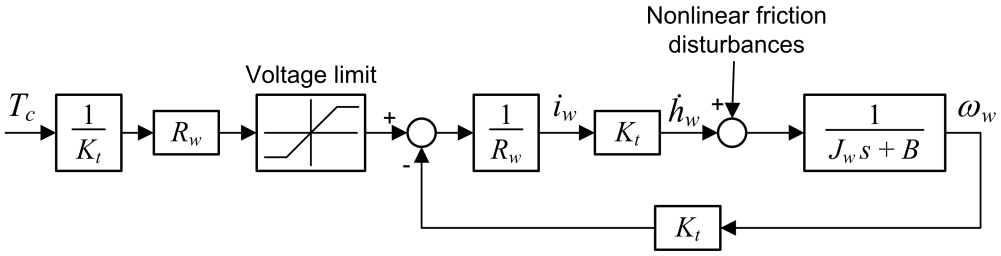

Figure 3. Electromechanical model of a reaction wheel.

is the electrical resistance of the motor armature; i_w is the motor current; $\dot{h}_w$ is the achieved inertial torque; ω_w is the flywheel angular velocity; J_w is the flywheel moment of inertia; and B_r is the viscous damping coefficient of the rotor.

Magnetic torqrods are reliable and cost efficient devices whose torque is generated through the interaction between the on-board electromagnetic dipole moment and the geomagnetic field. Likewise the reaction wheels, a physical setup of three magnetic torqrods aligned with the spacecraft principal axes has been assumed. The magnetic control torque is based on the principle of perpendicularity [8, 13] expressed as

$$\mathbf{T}_m = \mathbf{B}\mathbf{m} = \frac{1}{|\mathbf{b}|^2}\mathbf{B}\mathbf{B}'\mathbf{T}_c \tag{2}$$

where $\mathbf{m} \in \mathbb{R}^3$ is the magnetic dipole moment; and $\mathbf{B} \in \mathbb{R}^{3\times 3}$ is a matrix composed of the components of the Earth's magnetic field in the body reference frame, given by

$$\mathbf{B} = \begin{bmatrix} 0 & b_z & -b_y \\ -b_z & 0 & b_x \\ b_y & -b_x & 0 \end{bmatrix} \tag{3}$$

3. Proposed solution to the mixed actuators problem

Multiobjective optimization is mainly applied for solving conflicting problems in a systematical and simultaneous way. In this paper, the mixed actuators problem is solved using the proposed Actuator Multiobjective Command Method (AMCM) [4]. The multiobjective problem is formulated here with four objectives functions: torque error, fuel and electrical charge consumptions, disturbance of coupling, and risk of utilization. These objectives present conflicting behaviors, since satellite actuators have different characteristics, and should be simultaneously minimized. The first objective function, Z_1, measures the torque error: difference between the requested torque and the total applied torque. The second objective function, Z_2, expresses the total amount of propellant mass and electrical charge consumed by all actuators. The third objective function, Z_3, represents the actuator's disturbance effect on the satellite's axes. The last objective function, Z_4, denotes the failure probability of each set of actuators. These objectives functions compose the objective function vector, $\mathbf{Z}(\mathbf{x})$, and they measure, in a general way, the cost and efficiency of the actuators. The mathematical formulation of the multiobjective problem is given by

$$
\begin{aligned}
\text{Minimize} \qquad \mathbf{Z}(\mathbf{x}) &= [Z_1(\mathbf{x}), Z_2(\mathbf{x}), Z_3(\mathbf{x}), Z_4(\mathbf{x})] \\
\mathbf{x} &= \frac{\mathbf{p}}{k}|T_c| \\
\\
Z_1(x_1,x_2,x_3) &= T_r^a(x_1) + T_w^a(x_2) + T_m^a(x_3) - |T_c| \\
Z_2(x_1,x_2,x_3) &= c_1x_1 + c_2x_2 + c_3x_3 \\
Z_3(x_1,x_2,x_3) &= i_1x_1 + i_2x_2 + i_3x_3 \\
Z_4(x_1,x_2,x_3) &= r_1x_1 + r_2x_2 + r_3x_3 \\
\\
\text{subject to} \qquad x_1,x_2,x_3 &\geqslant 0 \\
p_1 + p_2 + p_3 &= k \\
\Rightarrow x_1 + x_2 + x_3 &= |T_c| \\
k &= \frac{\Delta h_c}{\Delta h_a}
\end{aligned}
\tag{4}
$$

where Δh_a is the actuator sample period; Δh_c is the controller sample period; k is the number of subsets; and T_c is the torque signal requested by the PID controller.

Combinatorial combinations of the requested torque compose the discrete decision variable vector, $\mathbf{x}$, whose components (x_1, x_2, x_3) represent the torque signal commanded to the actuators: RCS, reaction wheel, and magnetic torqrod, respectively. The coefficients c_j, i_j and r_j (with j = 1,2 and 3) are constant values used to establish the tradeoff among the objective functions. The combinatorial vector, $\mathbf{p} \in \mathbb{R}^n$, has the function of quantizing the torque signal in order to generate the set of decision variables. The k-combination with repetitions equation (also called by k-multicombinations) [14] is used to solve the combinatorial problem. This method calculates the number of ways to sample k elements from a set of n elements, allowing for duplicates, in a linear Diophantine equation. Therefore if a given set has n elements, then the number of such k-multisubsets is written as

$$\left(\begin{array}{c} n+k-1 \\ k \end{array} \right) = \frac{(n-1+k)!}{(n-1)!k!} \tag{5}$$

where, in this case, n represents the number of decision variables, i.e, the number of actuators ($n = 3$); and k is the number of divisions of the control cycle which is assumed here as $k = 10$, since the actuators model executes 10 times faster than the control cycle. Thus the set of candidate solutions has a finite amount of 66 elements.

The proposed AMCM needs to know a priori the error level of each actuator as a function of the candidate torque solution (x_1, x_2, x_3). Then curve fitting analysis of the actuators model has been performed in order to determine the actuators' torque response. Such equations consider the same nonlinearities parameters, like biases and random errors, of the actuators models. In Eq. 4, $T_r^a(x_1)$, $T_w^a(x_2)$, and $T_m^a(x_3)$ are the test torque theoretical functions of the RCS, reaction wheel, and magnetic torqrod, respectively, such as

$$T_r^a(x_1) = \begin{cases} T_r^{max} + \bar{w} & \text{for} \quad x_1 \geqslant T_r^{max} \\ x_1 + \bar{w} & \text{for} \quad 0 < x_1 < T_r^{max} \\ 0 & \text{for} \quad x_1 = 0 \end{cases} \tag{6}$$

$$T_w^a(x_2) = \begin{cases} x_2 + w + b_s & \text{for} \quad x_2 \leqslant T_w^{max} \\ T_w^{max} + w + b_s & \text{for} \quad x_2 > T_w^{max} \end{cases} \tag{7}$$

$$T_m^a(x_3) = \begin{cases} (a_m x_3^2 + b_m x_3) + w + b_s & \text{for} \quad x_3 \leqslant T_m^{max} \\ T_m^{max} + w + b_s & \text{for} \quad x_3 > T_m^{max} \end{cases} \tag{8}$$

where the superscript ^{max} represents the theoretical maximum torque applied by the actuator; w is the white Gaussian noises whose statistics is given by $w = N(0, Q)$, i.e., zero mean and covariance Q; b_s is the bias error; and a_m and b_m are the coefficients of a second degree polynomial that best fit the torque curve of the magnetic torqrod. The thruster's torque error is modeled considering the average torque error, $\bar{w}$, of the last 100 simulation steps.

When the multiobjective problem is solved, a set of optimal solutions, called in literature non-inferior set [15] or Pareto front [16], is found. The conflicting behavior among the objectives makes the optimal values have the same degree of optimality. However, sometimes it is necessary to select a single alternative from the set of optimal solutions. Then it is applied here the equilibrium method Smallest Loss Criterion (SLC) [17, 18, 19]. This approach selects a unique solution, called best compromise solution, $\mathbf{x}^b \in R^n$, without prioritize any objective function. Mathematically it relies on finding the barycenter - defined as the equilibrium point at the objective space - of a normalized

p-dimensional figure. The SLC evaluates the Euclidean distance from the barycenter to all candidate solutions and selects the closest candidate as the best compromise solution, such as

$$\mathbf{x}^b = \arg\{\min|\mathbf{Z}(\mathbf{x}) - \mathbf{Z}(\mathbf{x}^*)|\} = \min\left\{\sum_{1}^{p}[Z_i(\mathbf{x}) - Z_i(\mathbf{x}^*)]^2\right\}^{1/2} \tag{9}$$

where $\mathbf{x}^* \in \mathbb{R}^n$ is the barycenter solution. It is assumed here as the solution which optimizes simultaneously all objectives in a multiobjective problem

Figure 4 illustrates the multiobjective optimization process proposed in this paper to solve the mixed actuators problem. Firstly, the decision space is loaded according to the requested torque signal. Afterward all decision variables are tested in the actuators models in order to gather the feasible solutions. Then the objective functions are evaluated for every candidate solution. In the next step, the SLC decision making method selects the best compromise solution from the set of optimal solutions. Thus the selected solution is commanded to actuators and the loop is completed with the application of torque in the vehicle's dynamics model.

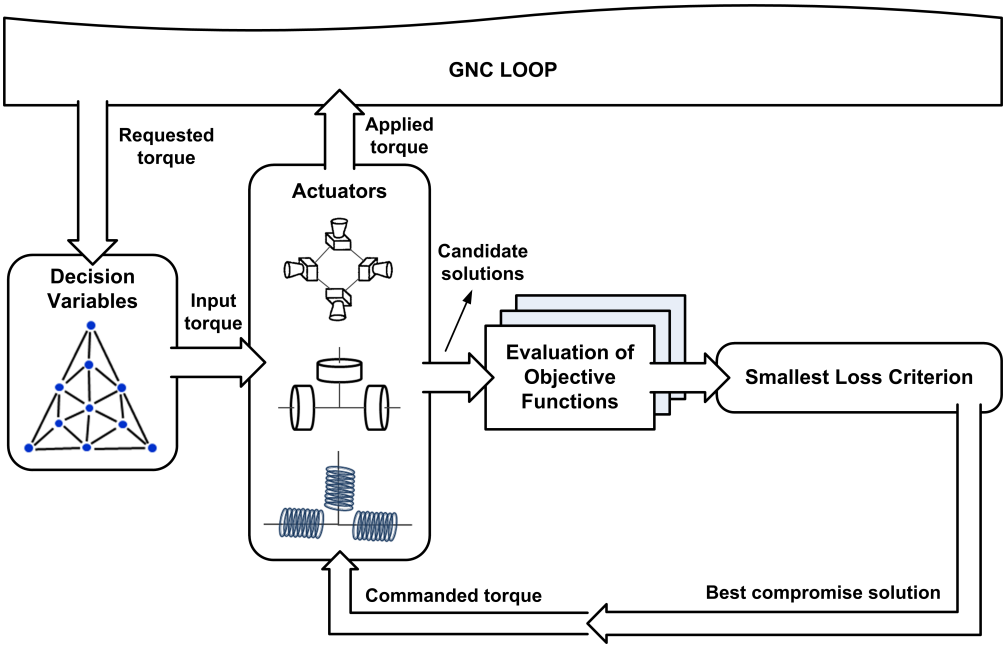

Figure 4. Multiobjective optimization process of AMCM.

4. Results

This section deals with purely numerical simulations as well as real-time simulations. In the former case, the proposed method has been compared to the single-actuators case and the multiobjective optimization process is evaluated. In the latter analysis, AMCM is tested in a HIL rendezvous and docking simulator. Both cases show the results of a final approach rendezvous from 20 m to 10 m. In addition, an attitude maneuver is concurrently executed to correct an initial angular error - difference between the actual attitude and the desired values - of 10 degrees along Y_B axis. The

main parameters of the simulation are presented in Tab. 1. The technical data of the actuators and sensors are realistic specifications based on data sheets of suppliers.

Table 1. Simulation parameters.

Orbit parameters	**Value**	**Multiobjective coefficients**	**Value**
Altitude, km	450	Fuel and electrical consumption (**c**)	[3, 2, 1]
Eccentricity	0	Disturbance of coupling (**i**)	[2, 1, 3]
Inclination, deg	45	Risk of utilization (**r**)	[1, 3, 2]
Mean anomaly, deg	90		
Satellite parameters		**RCS parameters**	
Moment of inertia, kg.m^2	[100, 120, 80]	Propellant	Cold gas
Initial mass, kg	500	Thrust, N	0.5 ; 1
Approach velocity, m/s	0.05	MIB, Ns	0.05 ; 0.1
Stellar attitude sensor		**Reaction wheel parameters**	
Spatial random error, arcsec.	18.9, 3σ	Wheel moment of inertia, kg.m^2	0.0191
Spatial bias error, arcsec.	10, 3σ	Maximum torque, Nm	0.054
Camera CCD sensor		**Magnetic torqrod parameters**	
Focal length, pixels	604	Magnetic dipole moment, Am^2	170
Resolution, pixels	640 x 480	Maximum torque*, Nm	0.012

* Achieved with the Earth's magnetic field of the particular orbital position.

4.1. Multiobjective optimization analysis

Firstly, the GNC loop has been simulated using the numerical models previously presented in Sec. 2. In this case, it is assumed thrusters with nominal thrust of 0.5 N. The value path representation [20] has been used to plot the objective space of the multiobjective problem. This representation, unlike graphical displays on orthogonal axes, allows considering simultaneously a large number of objectives. The value path plot for a given requested torque level (0.050 Nm) is illustrated in Fig. 5(a). The vertical axis represents the normalized scale of the objective functions whereas the horizontal axis comprises the parallel scales of each objective. The thick lines denote the optimal solution of each objective whereas the best compromise solution is represented by the dashed line. The remaining lines complete the set of candidate solutions. Note that a particular solution can optimize one objective but, on the other hand, provide the highest values for others objectives, like the optimal solution of Z_2. As discussed earlier, the decision variable represents combinatorial combinations of a torque signal commanded to the set of actuators. In this sense, the values of the best compromise solution, selected by AMCM in this particular control cycle, are exhibited in Fig. 5(b). Such values describe a percentage of the total amount of the requested torque. As can be seen, the major proportion of the commanded torque was requested from the reaction wheel (50%), followed by the RCS (30%) and magnetic torqrod (20%).

A complete numerical simulation of translational and rotation motions has been executed. Accordingly, the efficiency of AMCM has been evaluated through performance parameters of the GNC loop: angular error integrated over time, propellant mass consumption, electrical charge consump-

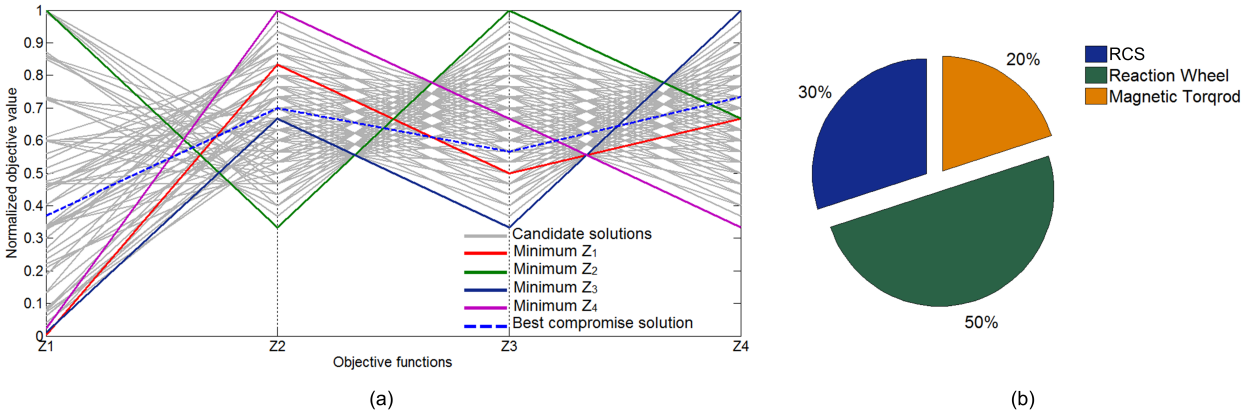

(a) (b)

Figure 5. Multiobjective analysis for a requested torque of 0.050 Nm: (a) objective space; (b) AMCM commanded torque.

tion, settling time of the angular response, and the normalized objective values of the disturbing of coupling and risk of utilization. In this case, the total time of simulation is 350 s. As shown in Fig. 6, each bar represents a different configuration of actuators. The first configuration uses RCS to control both translational and rotational motions. The second and third configurations use thrusters only for controlling the translational motion. Reaction wheels on the second configuration and magnetic torqrods on the third configuration are used to control the rotational motion.

Note that the proposed AMCM presented the second lowest angular error (4.28 deg.s); an acceptable amount of propellant mass consumption since the others results were similar; an intermediate value of electrical charge consumption (0.058 Ah); the fastest settling time among all configurations (86.47 s); and low levels of disturbance of coupling (0.16) and risk or utilization (0.27). The results have indicated that a better attitude control performance can be achieved with the proposed method compared to the single actuators mode.

4.2. HIL rendezvous simulations at EPOS facility

Integration, test and verification of the proposed method have been made at the robotic rendezvous simulator of the German Aerospace Center, called European Proximity Operations Simulator (EPOS). The translational and rotational motions of two docking satellites are controlled in real-time based on measurements of the real monochromatic camera sensor [7] (see Fig. 7). EPOS comprises two industrial robots in a separation ranging from 25 m to 0 m. The facility layout, illustrated in Fig. 7, has the Robot 1 mounted on a linear rail system and the Robot 2 mounted on a base at the end of the rail system in the laboratory. Both robots are commanded with 250 Hz command rate. EPOS also includes a PC-based real-time facility control system to monitor and control the HIL simulations [6].

Although the test campaign in EPOS has covered several phases, this paper presents just the relevant results of the final tests in closed-loop mode. The complete test campaign can be consulted in [4]. The primary objective of these tests was to check if stability conditions in a real-time environment could be achieved using the proposed AMCM for commanding the set of actuators. In this case,

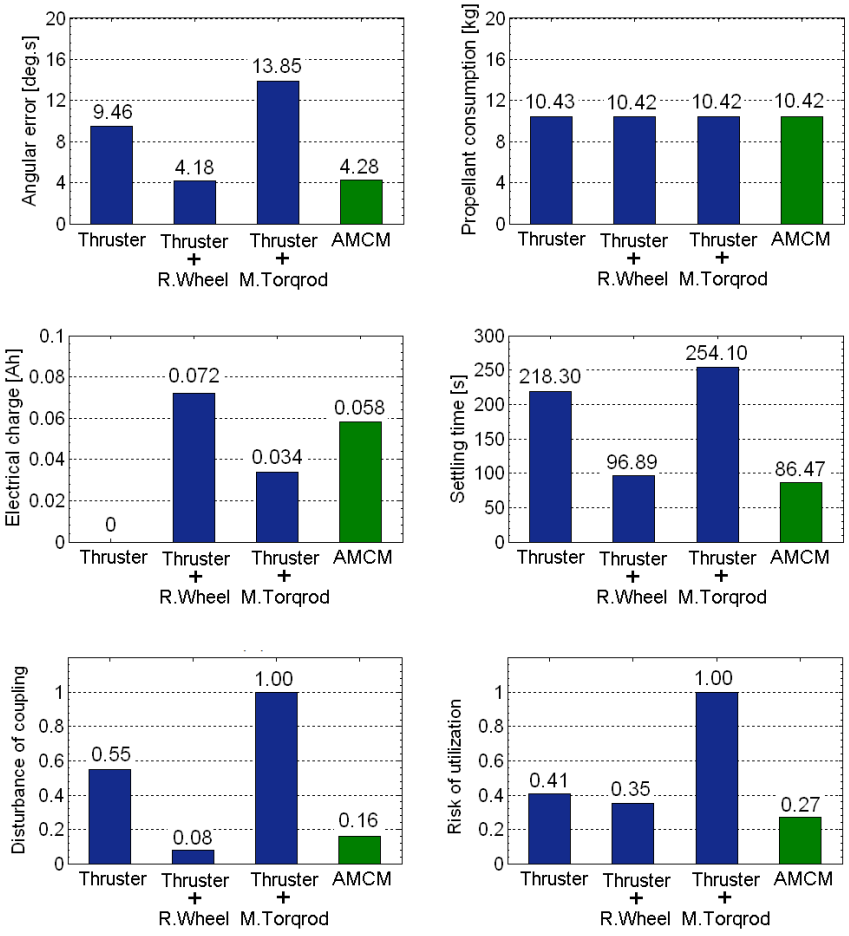

Figure 6. Performance parameters of the GNC loop.

Figure 7. The robots of the EPOS facility.

the RCS is composed of thrusters with nominal thrust of 1 N. In a closed-loop simulation, the output of the spacecraft's dynamics model is sent to the robots at every 4 ms. Then the visual camera sensor measures the robot position with respect to the camera and send this information to the image processing algorithm [21] with an update rate of 5 Hz. After processing it, the data is smoothed by a navigation filter [7], compared to a reference trajectory, and, based on this error, a

control signal is handed over by the controller to the AMCM model which will optimally command the actuators. The loop is closed with the application of the necessary force and torque to the spacecraft's dynamics model.

Figure 8 presents the translational (left) and rotational (right) motions of the robots as function of time. Such motions represent the relative state in the CLW coordinate frame. Firstly, the GNC loop is analyzed at a hold point of 20 m using an ideal sensor (null measurement errors). Then the pinhole camera model is activated. Afterward the real camera starts to be used in the GNC loop for measuring the relative position. Around the simulation time 500 s starts the rotational motion which turns out in a reduction of the error along Y_B axis. The continuous approach maneuver is initialized around the simulation time 800 s and it takes about 200 s. The rotational motion is performed in approximately 40 s. As can be seen in Fig. 8, the proposed GNC loop was able to accomplish the complete translational and rotational maneuver ensuring the stability conditions of the system.

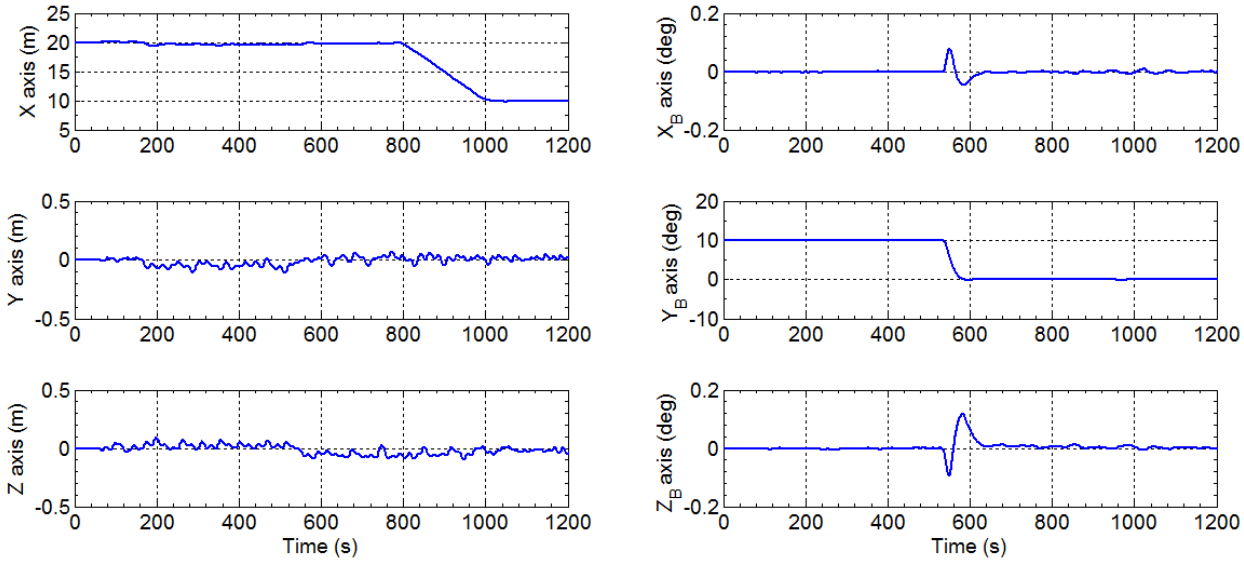

Figure 8. Translational (left) and rotational (right) position as a function of time.

5. Conclusions

In this work, a novel solution for the mixed actuators problem based on a multiobjective optimization technique has been proposed. The decision space is created in terms of combinatorial combinations of the control signal. This approach allows generating a set of candidate solutions which simultaneously minimize a group of four objective functions. Nevertheless, since the algorithm should operate online and autonomously, a decision making method selects the best compromise solution from the Pareto front. The conflicting behavior of the objective functions has been studied and discussed in this paper. Accordingly, the AMCM model has been included in a complete GNC loop and evaluated in both numerical and real-time simulations. The analysis of the control system's performance parameters have indicated that a mixed actuators mode, commanded by AMCM, achieved a low level of angular error, satisfactory amount of fuel and electrical charge consumptions, low levels of disturbing of coupling and risk of utilization, with the fastest settling time of angular response, when compared to the other single-type actuators configurations. In addition, HIL rendezvous simulations

have evidenced that the proposed models can properly operate in a real-time environment.

Acknowledgments

This research was sponsored by CAPES Foundation, Ministry of Education of Brazil, process number BEX 3512/13-4. The authors also wish to thank the German Aerospace Center (DLR) and the National Institute for Space Research (INPE) which provided all the necessary support for the development of the work.

6. References

[1] Bruno, D. "Contigency Mixed Actuator Controller Implementation for the Dawn Asteroid Rendezvous Spacecraft." "Proceedings...", Conference and Exposition, AIAA, Pasadena, 2012.

[2] Macala, G. A., Lee, A. Y., and Wang, E. K. "Feasibility Study of Two Cassini Reaction Wheel/Thruster Hybrid Controllers." Journal of Spacecraft and Rockets, Vol. 51, No. 2, pp. 574–585, 2014.

[3] Dennehy, C. J. "Spacecraft Hybrid (Mixed-Actuator) Attitude Control Experiences on NASA Science Missions." "Proceedings...", International ESA Conference on Guidance, Navigation & Control Systems, ESA, Porto, 2014.

[4] Santos, W. G. Discrete Multiobjective Optimization applied to the Spacecraft Actuators Command Problem and Tested in a Hardware-in-the-loop Rendezvous Simulator. Thesis (doctorate in space engineering and technology), National Institute for Space Research (INPE), São José dos Campos, 2015.

[5] Fehse, W. Automated rendezvous and docking of spacecraft. Cambridge University Press, Cambridge, UK, 2003.

[6] Boge, T., Benninghoff, H., and Tzschichholz, T. "Hardware-in-the-loop Rendezvous Simulation Using a Vision Based Sensor." "Proceedings...", International ESA Conference on Guidance, Navigation and Control Systems, ESA, Karlovy, 2011.

[7] Benninghoff, H., Rems, F., and Boge, T. "Development and Hardware-in-the-loop Test of a Guidance, Navigation and Control System for On-orbit Servicing." Acta Astronautica, Vol. 102, pp. 67–80, 2014.

[8] Sidi, M. J. Spacecraft dynamics and control. Cambridge University Press, Cambridge, UK, 1997.

[9] Kristiansen, R. and Hagen, D. "Modelling of Actuator Dynamics for Spacecraft Attitude Control." Journal of Guidance, Control, and Dynamics, Vol. 32, No. 3, pp. 1022–1025, 2009.

[10] Tewari, A. Atmospheric and space flight dynamics. Birkhauser Boston, New York, USA, 2007.

[11] Hartley, R. and Zisserman, A. Multiple view geometry in computer vision. Cambridge University Press, Cambridge, UK, 2004. 2nd ed.

[12] Åström, K. J. and Wittenmark, B. Computer-controlled systems. Prentice Hall, Beijing, China, 1997. 557 p.

[13] Silani, E. and Lovera, M. "Magnetic Spacecraft Attitude Control: A Survey and Some New Results." Control Engineering Practice, Vol. 13, No. 3, pp. 357–371, 2005.

[14] Brualdi, R. A. Introductory combinatorics. Pearson Education, New York, 1992.

[15] Cohon, J. L. Multiobjective programming and planning. Dover Publications, Mineola, NY, 2003.

[16] Pareto, V. Manuale de economia politica. Societa Editrice Libraria, New York, 1992. Translated into English by A. S. Schwier as "Manual of political economy", edited by A. S. Schwier and A. N. Page, A.M. Kelley.

[17] Rocco, E. M., Souza, M. L. O., and Prado, A. F. B. A. "Multi-objective Optimization Applied to Satellite Constellations I: Formulation of the Smallest Loss Criterion." "Proceedings...", International Astronautical Congress, IAC, Bremen, 2003.

[18] Rocco, E. M., Souza, M. L. O., and Prado, A. F. B. A. "Further Application of the Smallest Loss Criterion in the Multi-objective Optimization of a Satellite Constellation." "Proceedings...", pp. 3165–3172. International Astronautical Congress, IAC, Fukuoka, 2005.

[19] Rocco, E. M., Souza, M. L. O., and Prado, A. F. B. A. "Station Keeping of Constellations Using Multiobjective Strategies." Mathematical Problems in Engineering, Vol. 2013, pp. 1–15, 2013. doi:10.1155/2013/476451.

[20] Schilling, D. A., Revelle, C., and Cohon, J. "An Approach to the Display and Analysis of Multiobjective Problems." Socio-Economic Planning Sciences, Vol. 17, No. 2, pp. 57–63, 1983.

[21] Tzschichholz, T., Boge, T., and Benninghoff, H. "A Flexible Image Processing Framework for Vision-based Navigation using Monocular Imaging Sensors." "8th International ESA Conference on Guidance, Navigation & Control Systems," p. 15. Karlovy Vary, Czech Republic, 2011.